Morphological Comparison of Axenic Amastigogenesis of Trypomastigotes and Metacyclic Forms of *Trypanosoma cruzi*

María C Navarro, Ana R De Lima, José Askue*, Víctor T Contreras/+

Laboratorio de Protozoología, Centro BioMolP, Facultad de Ciencias de la Salud, Universidad de Carabobo, Valencia, Estado Carabobo, Venezuela *Facultad de Agronomía, Universidad Central de Venezuela, Maracay, Estado Aragua, Venezuela

Amastigogenesis occurs first when metacyclic trypomastigotes from triatomine urine differentiate into amastigotes inside mammalian host cells and a secondary process when tissue-derived trypomastigotes invade new cells and differentiate newly to amastigotes. Using scanning electron microscopy, we compared the morphological patterns manifested by trypomastigotes and metacyclic forms of Trypanosoma cruzi *during their axenic-transformation to amastigotes in acidic medium at 37°C. We show here that in culture MEMTAU medium, secondary and primary axenic amastigogenesis display different morphologies. As already described, we also observed a high differentiation rate of trypomastigotes into amastigotes. Conversely, the transformation rate of in vitro-induced-metacyclic trypomastigotes to amastigotes was significantly slower and displayed distinct patterns of transformation that seem environment-dependent. Morphological comparisons of extracelullar and intracellular amastigotes showed marked similarities, albeit some differences were also detected. SDS-PAGE analyses of protein and glycoprotein from primary and axenic extracelullar amastigotes showed similarities in glycopeptide profiles, but variations between their proteins demonstrated differences in their respective macromolecular constitutions. The data indicate that primary and axenic secondary amastigogenesis of* T. cruzi *may be the result of different developmental processes and suggest that the respective intracellular mechanisms driving amastigogenesis may not be the same.*

Key words: *Trypanosoma cruzi* - primary amastigogenesis - secondary amastigogenesis - differentiation processes

Trypanosoma cruzi, the etiological agent of Chagas disease is a Stercorarian trypanosome, transmitted as infective metacyclic trypomastigotes to mammalian host via the feces or urine of the insect vector. Flagellated trypomastigotes are ingested by vertebrate cells through a process referred to as parasite-directed endocytosis (Burleigh & Andrews 1995) with formation of a parasite-containing endocytic vacuole which fuse with lysosomes from the host cell (Carvalho & De Sousa 1989, Tardieux et al. 1992). Within 2 h after infection, the trypomastigotes can leave the acidic environment as a phagosome before the transformation into amastigotes is completed (Ley et al. 1990) and enter the slightly alkaline environment of the cytoplasm, where they multiply as aflagellate amastigotes (Burleigh & Andrews 1995). These early events appear to occur at different rates depending on the type of vertebrate cells studied. It has been shown by optical microscopy that following vertebrate cell penetration, metacyclic trypomastigotes reorganize into amastigotes (in about 3 h) and remain morphologically quiescent in a lag period within the cell for about 35 h (at 35°C) prior to the onset of reproduction (Dvorak 1975). It has been proposed that the lag period observed, at least in part, must represent the time necessary for their transformation into amastigotes (Ley et al. 1988). The amastigotes then divide and transform into trypomastigotes. Upon leaving the cell, the tissue-derived trypomastigotes enter the bloodstream, and are capable of infecting surrounding cells or disseminate to other tissues via the bloodstream, repeating the intracellular events. The tissue-derived trypomastigotes can be eventually taken up by the insect host. In the intestine of the invertebrate host the blood trypomastigotes transform into epimastigotes. The epimastigotes then divide and give rise to infective metacyclic trypomastigotes. Consequently, a primary amastigogenesis occurs when metacyclic trypomastigotes from triatomine urine differentiate into amastigotes inside mammalian host cells, and a secondary process is observed when tissue-derived trypomastigotes differentiate into amastigotes.

Most of the information concerning the in vitro and in vivo amastigogenesis process comes from the study of tissue-derived trypomastigote forms (Nogueira & Cohn 1976, Milder et al. 1977, Ley et al. 1988, Burleigh & Andrews 1995, Barros et al. 1996, 1997), but little is known about the developmental process driving the metacyclic forms to amastigotes. Although, metacyclic trypomastigotes can appear similar in morphology and share some biological properties with tissue-derived trypomastigotes. However, the latter has the capacity to transform into epimastigotes at 27°C in blood or axenic medium, a property that is absent in metacyclic trypomastigotes (Brener 1973). Both forms also have stage-specific antigens and they display different modes of interaction with host cells (Burleigh & Andrews 1995). For instance, metacyclic trypomastigotes express on their

This research was supported by grants from Fonacit S1-97000664 (VTC, ARDL), Fonacit S1-2001000683 (MCN, VTC, ARDL), Codecih FCS-97018 (ARDL, VTC) and Codecih FCS-99010 (MCN VTC).

Corresponding author. Present address: VLN 1500 PO Box 025685, Miami, Fl, 33102-5685 USA
Fax: +58241-8673342. E-mail: convictu@cantv.net.ve

Received 27 May 2002
Accepted 15 October 2002

surface several glycoproteins that interact with mammalian cells, which have no counterpart in blood trypomastigotes (Ruiz et al. 1993).

Using axenic conditions, several investigators have reported the morphological differentiation of bloodstream trypomastigotes into amastigotes and the morphological and ultrastructural changes throughout transformation have been described (Villalta & Kierzenbaum 1982, Andrews et al. 1987, Kambara et al. 1990, Tomlinson et al. 1995). In a carefully performed work, Andrews et al. (1987) studied the morphological transformation by transmission electron microscopy (SEM), of tissue-culture derived trypomastigotes into amastigotes and described a complex pattern of morphological rearrangements which occurred during 24 to 48 h of incubation and found that the morphological changes were associated with the expression of specific membrane antigens. Tomlinson et al. (1995) confirmed by SEM and antigenic analysis that the incubation at 37°C of tissue-culture derived trypomastigotes in acidic media accelerated greatly the morphological transformation, which was also accompanied by the acquisition and loss of specific membrane antigens. Other authors have obtained extracelullar round amastigote-like forms from metacyclic trypomastigotes using highly enriched media (Kimura et al. 1978, Pan 1978, Rondinelli et al. 1988). Taking these observations together along with the little attention given to comparative morphology between the transformation of trypomastigotes and metacyclic forms into amastigotes raised the question of whether both transformations occurred following similar or different developmental patterns.

To address this question, we have studied by SEM the morphological events that occur during the primary and secondary amastigogenesis of *T. cruzi*. Furthermore, we have compared intracellular amastigotas with their corresponding extracellular amastigotes.

MATERIALS AND METHODS

Parasites and stages - Throughout this study, cloned EPm6 isolate of *T. cruzi* was used. The parasite was cloned and maintained by alternate triatomine/mouse passages as previously described (Contreras et al. 1994). The procedures to obtain in vitro-induced metacyclic and extracelullar-derived metacyclic amastigotes were described in details previously (Contreras et al. 2002).

In vitro primary amastigogenesis - The transformation kinetic to produce extracellular-amastigotes from in vitro-induced metacyclic trypomastigotes (EMA) was described (Contreras et al. 2002). In brief, DEAE-52-purified metacyclic trypomastigotes were transferred to sterile plastic tissue culture flasks (175 cm^2 Falcon Labware, Oxnar, CA) containing 14 ml of MEMTAU medium pH 5.8, which consists of a 1:1 mixture of TAU3AAG medium and MEM 10% FBS medium, supplemented with 70 mM Sucrose, 20 µg/ml bovine or human Hemoglobin, 200 U/ml Penicillin, 200 µg/ml Streptomycin, and 20 mM MES [2 (N-morpholinoethanesulfonic) acid hydrate], followed by incubation at 37°C, without agitation in a 5% CO_2 atmosphere for one, two or three days, namely as pre-incubation phase. After three days of pre-incubation, the parasites were centrifuged, resuspended, transferred to sterile culture flasks and incubated for one, two or three days under the same conditions described above, namely as the re-incubation phase.

In vitro secondary amastigogenesis - Extracellular derived-trypomastigote amastigotes (ETA) were obtained essentially as described by Tomlinson et al. (1995) except by incubating in MEMTAU medium. Tissue-culture trypomastigotes from infected Vero cells were concentrated by centrifugation and resuspended in MEMTAU medium at 37°C, without agitation in a 5% CO_2 atmosphere for 3, 6, 9, 12, 18 and 24 h.

In vitro intracellular amastigotes - Intracellular-derived-metacyclic amastigotes (IMA) and intracellular-derived-trypomastigote amastigotes (ITA) were obtained by disruption of infected Vero cells prior to trypomastigogenesis, i.e., approximately three days after the infection of the monolayers with in vitro induced-metacyclic trypomastigotes or tissue-culture trypomastigotes, respectively. Infected monolayers were gently trypsinized, and the detached cells were recovered by centrifugation and resuspension in PBS (0.15M sodium chloride, 0.02M sodium phosphate, pH 7.2) supplemented with 1% BSA (Bovine Serum Albumin) (PBS-BSA). A 10 ml aliquot of the resuspension was disrupted by passage through a 25-gauge needle (Piras et al. 1982). The intracellular amastigotes were separated from the cell debris by centrifugation in a 15-21% discontinuous Metrizamide gradient (Carvalho & De Souza 1983).

SEM - Purified metacyclic trypomastigotes (day 0), pre-incubated (days 1, 2 and 3), re-incubated (days 1, 2 and 3), IMA, ITA, trypomastigotes (0 h) and from different times of incubation (3, 6, 9, 12, 18 and 24 h) were analyzed by SEM. Sample processing was carried out essentially as described by Andrews et al. (1987) using glass coverslips precoated with 10 µg/ml poly-L-lysine. Glutaraldehyde-fixed parasites were post-fixed with 1% OsO_4 in sodium cacodylate buffer, dehydrated in graded ethanol and critically point dried from liquid CO_2. Specimens were coated with gold-palladium in a BAL-TEC SCD050 evaporator before being examined in a Philips XL-20 scanning electron microscopy.

Analysis of polypeptides and glycopeptides by SDS-PAGE - EMA and ETA proteins were analyzed by SDS-PAGE (Laemmli 1970) on 10% uniform polyacrylamide slab minigels. Wells were loaded with 7 µg of protein. The resulting protein patterns were stained with a combined Coomassie Blue-Silver staining procedure (De Moreno et al. 1985) for proteins and combined Periodic Acid-Alcian Blue-Glutaraldehyde-Silver (PAABGS) stain procedure for glycoproteins (Dubray & Bezard 1982, Moller et al. 1993, Moller & Poulsen 1995). For glycoproteins, two types of markers were run in the same gel: the broad molecular weight range was used to estimate molecular weight and control the reversal of silver staining (unstaining) of proteins and a mixture of proteoglycans and glycoproteins (6 µg/well). The following glycoconjugates were used: Chondroitin 6-Sulfate from shark cartilage (type C, Sigma C-4384), Mucin from bovine sub maxillary glands (type I-S, Sigma M-3895), Fetuin from fetal calf serum (Sigma F-2379), and Bovine α-Acid Glycoprotein (orosomucoid, Sigma G-9014). The gels were then scanned

in a Bio-Rad Imaging Densitometer, model GS-690, and their profiles were analyzed using the Bio-Rad Molecular Analyst®/PC 1.2 software package.

RESULTS

In vitro transformation of tissue-culture derived trypomastigotes into amastigotes - A detailed morphological analysis of the extracellular differentiation kinetic of tissue culture-derived trypomastigotes into amastigotes was carried out using SEM. Parasites released at the third day after infection from Vero cells in culture showed a typical trypomastigote bloodstream morphology (Fig. 1a), characterized by C- or S-shaped, thick and elongated bodies (total length 12. 88 ± 1.98 µm; main width 1.19 ± 0.20), prominent kinetoplast terminal or sub-terminal (1.47 ± 0.48 µm from posterior end, arrow Fig. 1a), thick moderate to long flagella and a conspicuous undulating membrane. When these parasites are incubated in MEMTAU medium at 37°C, an accelerated appearance of forms resembling amastigotes occurs within 24 h (Fig. 1b-j). Within 3 h of incubation, broad trypomastigotes (Fig. 1b) and parasites with twisted body and sharp posterior cell end (Fig. 1c) were detected. At 6 h, it was possible to observe a progressive sinking of the flagellum into the cytoplasm of the parasites (Fig. 1d-e) maintaining sharp the posterior cell end. At 9 h of incubation, the parasites present a nut-shaped morphology with longitudinal cracks and short free flagellum (Fig. 1f). In the next 12 h the parasite body fold around itself in helical fashion and an increasing degree of internalization of the flagellum can be seen (Fig. 1g). Between 18 (Fig. 1h) and 24 h of incubation, typical amastigotes became predominant and the transformation process accomplished (Fig. 1i-j). During the transformation process, different types of trails were released by the parasites, as described in the legend to Fig. 1.

Comparing ETA from 24 h of incubation (Fig. 1i-j) to their corresponding ITA isolated by Metrizamide gradient (Fig. 1k-l), a remarkable, gross morphological similarity can be seen. The bodies of both types of amastigotes are rounded or oval-shaped, have longitudinal cracks and a short protruding flagellum. However, their surface membranes display differences: ITA presents a smooth surface, while ETA exhibits a finely grained surface.

In vitro transformation of metacyclic trypomastigotes into amastigotes - With the aim of looking at the overall aspect of parasites during the transformation process, we examined the differentiating cells by SEM (Figs 2, 3). The TAU3AAG-purified parasites of the pre-incubation phase show a typical morphology of metacyclic trypomastigotes (Fig. 2a-b), characterized by a long and slender body (total length 20.02 ± 0.51 µm; main width 1.28 ± 0.25) slightly curved or S-shaped, sub-terminal kinetoplast (3.83 ± 0.76 µm from posterior end, arrows Fig. 2a-b), a thick flagellum edging the body of the parasite, with or without very short free flagellum. When these parasites are transferred from 27 to 37°C and maintained in MEMTAU medium for 1, 2 or 3 days, they do not transform to amastigotes, but morphological alteration were observed in the trypomastigote morphology (Fig. 2c-h). During the first day of pre-incubation, almost all of the metacyclic trypomastigotes display a slight lengthening and thinning (total length 21.41 ± 4.99 µm; main width 1.09 ± 0.26), showing a small-sized kinetoplast usually very far from its pointed posterior end (4.95 ± 1.06 µm from posterior end, arrows Fig. 2c-d), and a poorly-developed undulating membrane. A similar morphological pattern was observed on the second day of pre-incubation, though the total length and width of the parasites was reduced (16.51 ± 3.44 and 0.97 ± 0.17 µm, respectively) having a variable kinetoplast sub-terminal (5.13 ± 1.29 µm from posterior end, large arrows Fig. 2e-f). This morphology is notably kept in parasites pre-incubate by three day, except by a progressive shortening of the entire organism (total length 12.03 ± 3.03 µm; main width 0.65 ± 0.13), with an inconspicuous undulating membrane (Fig. 2g-h).

Although notable cellular rearrangements were not observed during the pre-incubation phase, the metacyclic trypomastigotes exhibited a lengthening followed by a shortening of the body as the pre-incubation time progressed (Fig. 2c-h). This enlargement process can be seen to initiate by a sharpening at either the posterior or anterior end of the parasites (Fig. 2c-d, short arrows), while the shortening process seems to occur preferentially by a sloughing off of the surface membrane from the posterior end of the parasite (Fig. 2e, g, h, arrowheads). This process is accompanied by a continuous loss of surface membrane, the lengthening at the posterior end and the slenderness of the metacyclic trypomastigote along with the release of a barely-visible material (Fig. 2c, f, short arrows). Moreover, small flagellar swellings, protruding from the flagellum at different levels and membrane blobbing were seen in some instances along the entire surface of the parasites (Fig. 2e, short arrows).

When MEMTAU-purified metacyclic trypomastigotes were re-incubated in fresh MEMTAU medium at 37°C, an accelerated appearance of forms resembling amastigotes occurs in the subsequent 72 h (Fig. 3). This phase of the transformation process was not synchronic, but the decrease in the proportion of metacyclic trypomastigotes was compensated by an increase of amastigotes and a decrease of differentiating forms. Within the first 8 to 24 h, visual inspection of the micrographs (Fig. 3a-b) suggests that from the start the metacyclic trypomastigotes begin to shorten at the posterior end leading to the formation of parasites of lesser length (total length 12.03 ± 3.03) with a terminal or sub-terminal kinetoplast (2.3 ± 0.70 µm from posterior end, Fig. 3a, arrow) and without a conspicuous undulating membrane. Subsequently, the entire parasite undergoes a rapid shortening showing a blunt posterior cell end, while the broad-end of the parasite is seen to fold around itself in helical fashion with a gradual internalization of the flagellum (Fig. 3c-d). The transformation process was completed in the next 48-72 h of re-incubation when a homogenous population of round forms displaying short protruding flagella could be seen (Fig. 3e-h). This second phase of the transformation (Fig. 3a-h) also was accompanied by the release of parasite trails, as described in the legend to Fig. 3.

The comparison of IMA isolated by Metrizamide gradient (Fig. 3i-j) with their corresponding EMA shows a notable gross morphological similarity, yet display differences on their membrane (Fig. 3g-h). While, the EMA exhibit a

rough surface membrane and longitudinal cracks, the IMA present a smooth, granulose and slanting crack on their surfaces. However, both type of amastigotes are rounded or oval-shaped and have a short protruding flagellum.

Protein and glycoprotein's patterns from EMA and ETA - Total protein patterns of the two amastigote types were visualized by Coomassie Blue-Silver as shown in Fig. 4A. As can be seen, ETA and EMA show polypeptide patterns of different molecular weight and intensity, even though both profiles appear to share many of the detected bands (Fig. 4A). In contrast, the glycopeptide patterns obtained by PAABGS of EMA and ETA are al-

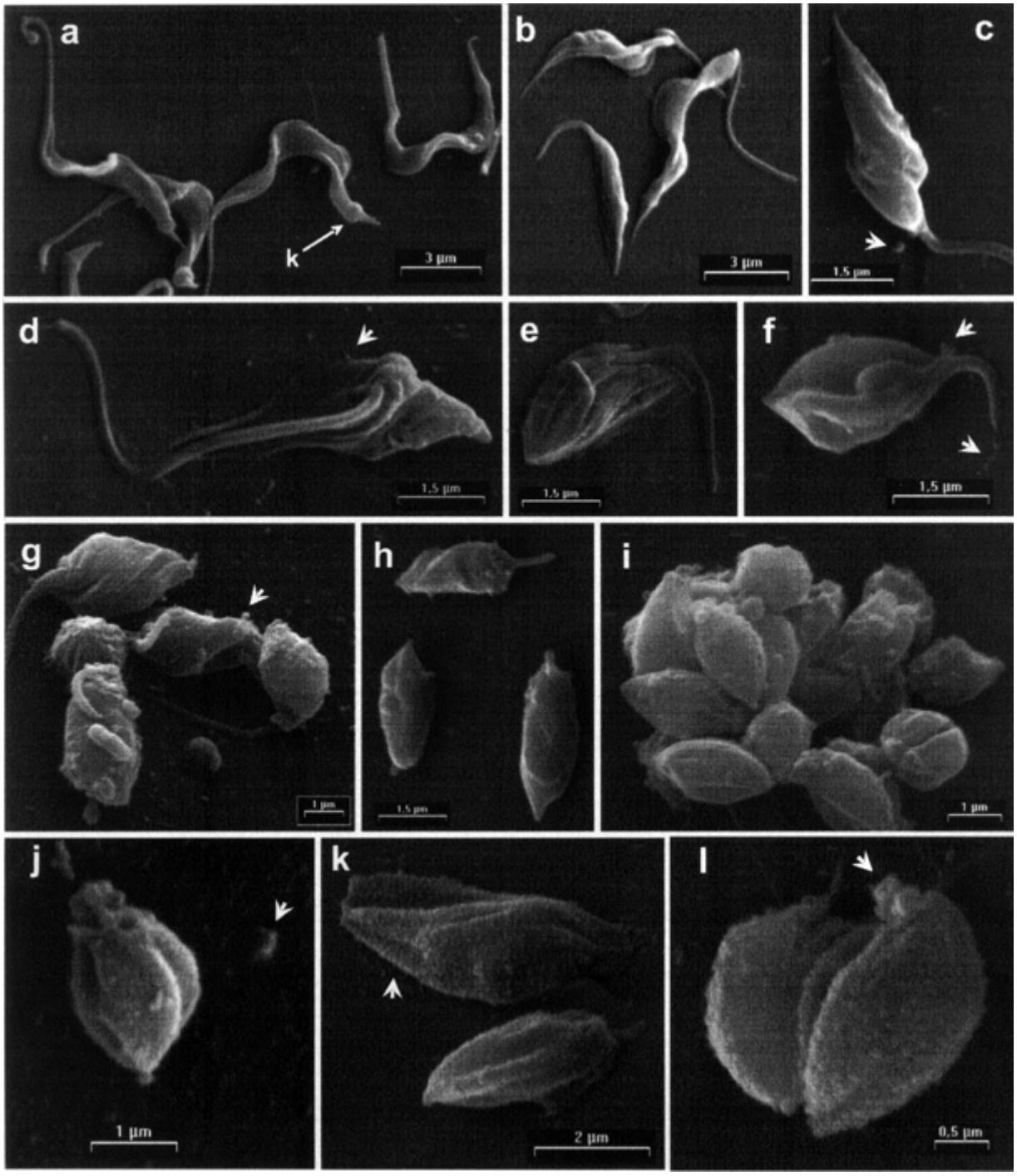

Fig. 1: scanning electron micrograph of *Trypanosoma cruzi* during the extracellular transformation of trypomastigotes to amastigote in MEMTAU medium at 37°C. Tissue culture trypomastigotes from the supernatant of Vero monolayer (a) before of the incubation in acidic medium present variable morphologies. After 3 (b, c), 6 (d, e), 9 (f), 12 (g), 18 (h) and 24 h (i, j) of incubation an accelerated cellular rearrangement can be observed. Arrow in a indicate a terminal kinetoplast (k). Morphological changes were accompanied by release of trails like-bead associated with the parasite (short arrows in d, f, g, j, k, l). Short arrows in f point to other type of trails being released at anterior end and the flagellum tip of the parasite. Short arrow in k and l indicate different type of trails being released by intracellular trypomastigote-derived amastigotes obtained by disruption of infected Vero cells.

most indistinguishable from each other (Fig. 4B), with ETA displaying higher glycopeptides complexity (lane ETA vs lane EMA, Fig. 4B). These results indicate that ETA and EMA are very similar in their glycoprotein content but differ substantially in their protein profile.

DISCUSSION

Trypanosomes are organism in which shape is dictated, at least in part, by the subpellicular array of microtubules that are cross-linked to each other and to the plasma membrane through MAPs (Gull 1999). It has been

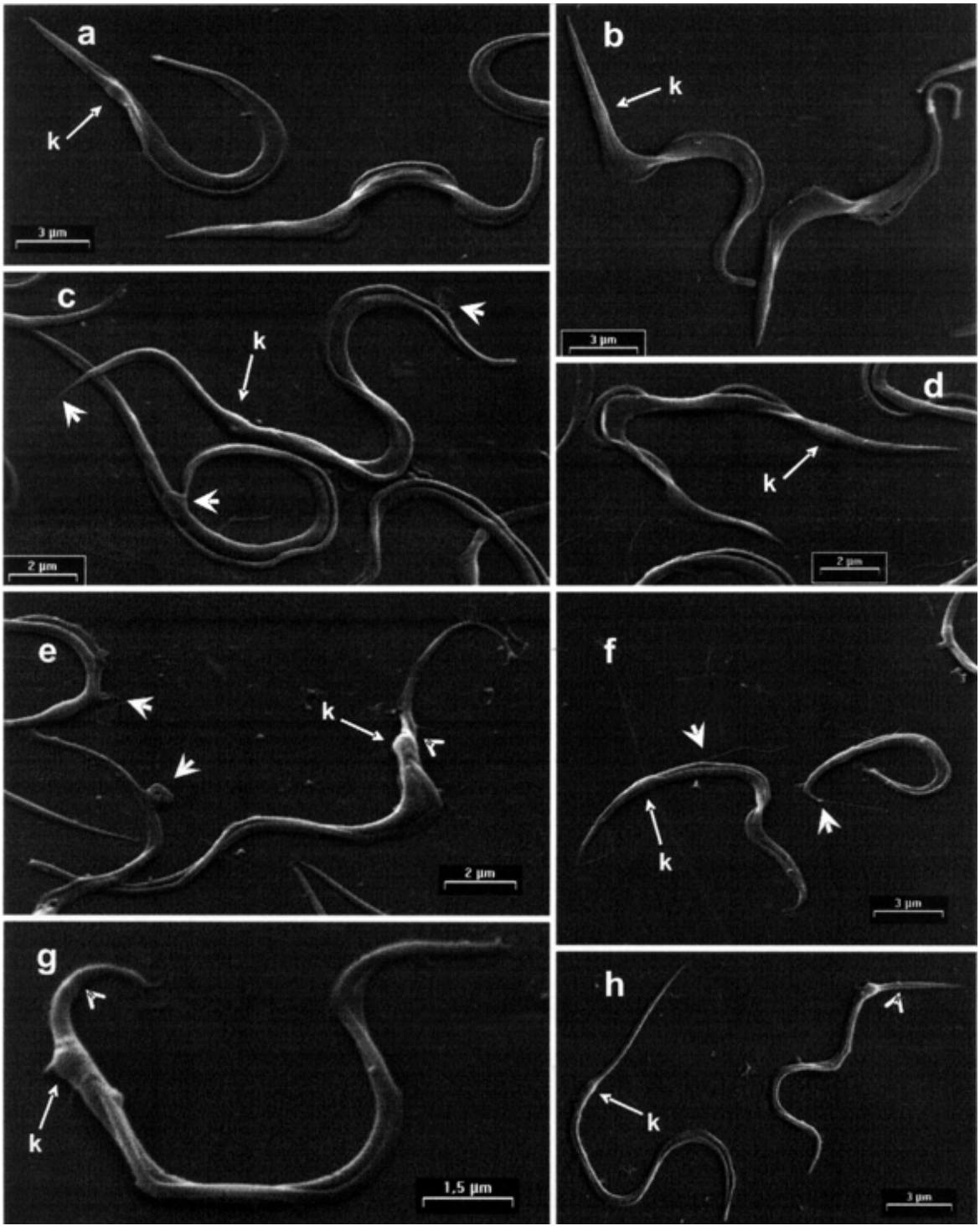

Fig. 2: scanning electron micrograph of *Trypanosoma cruzi* during the extracellular transformation of metacyclic forms to amastigotes. DEAE-purified metacyclic trypomastigotes (a, b) before of the pre-incubation phase. When these parasites are transferred from 27 to 37°C and maintained in MEMTAU medium for 24 (c, d), 48 (e, f) or 72 h (g, h), they do not transform to amastigote but the morphological changes occur under the trypomastigote morphology (c-h). These changes are accompanied by release of different type of trails associated with the parasite (short arrows in c, e, f). Large arrows point to the variable sub-terminal position of the kinetoplast (k). Arrowheads in e, g and h indicate the fracture regions suggesting a sloughing off the surface membrane of the parasite.

emphasized that the extreme morphological and motility differences of the trypomastigote and amastigotes stages of *T. cruzi* offer an excellent chance to study microtubules-based mechanism of morphological control which would be difficult to discern in systems where such change is more subtle (Gull 1999, Tyler & Engman 2001). We have shown by SEM that in axenic conditions the morphological transformation of the tissue-cultured trypomastigotes and the in vitro-induced amastigotes from metacyclic trypomastigotes are different. The comparison of extracelullar and intracellular amastigotes morphology showed that they share many similarities but are not mor-

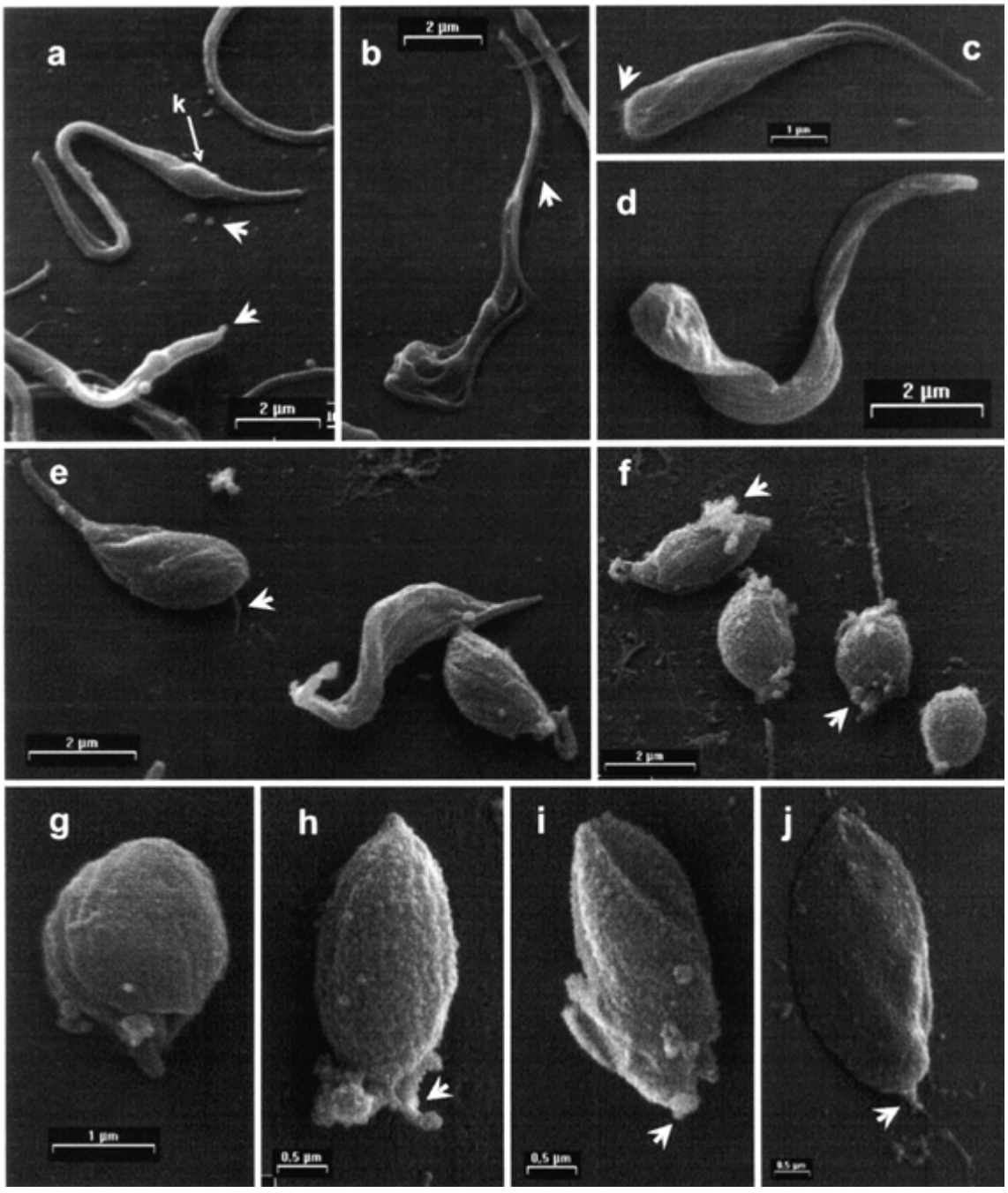

Fig. 3: scanning electron micrograph of *Trypanosoma cruzi* during the extracellular transformation of metacyclic to amastigote. When metacyclic trypomastigotes are re-incubated in fresh MEMTAU medium at 37°C for 8 (a, b), 24 (c, d), 48 (e, f) or 72 h (g, h) a notable cellular rearrangement can be observed. Large arrow in a indicate a prominent subterminal kinetoplast (k). The morphological changes are accompanied by release of different type of trails associated with the parasite (short arrows). Short arrows in c, e and f point to different type of trails being released at either the posterior or anterior end of the parasites. Short arrows in i and j point to different type of trails being released by intracellular metacyclic-derived amastigotes obtained by disruption of infected Vero cells.

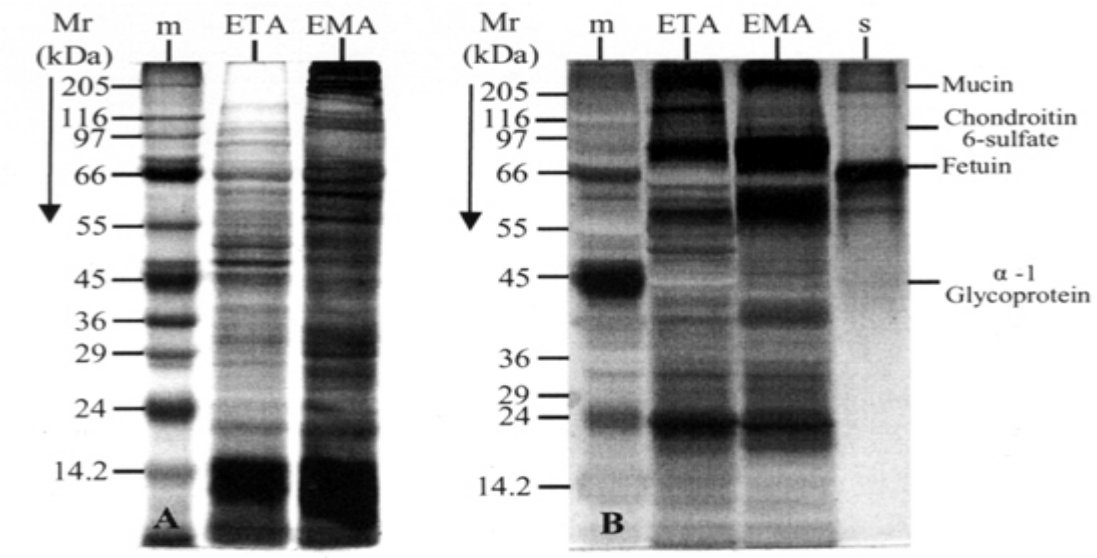

Fig. 4: SDS-10% PAGE analysis of extracellular amastigotes of *Trypanosoma cruzi*. The gels (6 µg/well) were stained with a combined Coomassie Blue-Silver stain procedure for proteins (A) or with a combined Periodic Acid-Alcian Blue-Glutaraldehyde-Silver (PAABGS) stain procedure for glycoproteins (B) as described into Materials and Methods. EMA corresponds to extracellular metacyclic-derived amastigotes and ETA to extracellular trypomastigote-derived amastigotes. Lanes m shows molecular weight markers and s a mixture of glycoproteins (6 µg) for controlling staining procedure. The numbers on the left side correspond to relative mobility (Mr) of the markers in kilodaltons (kDa).

phologically identical. The comparison of protein and glycoprotein profiles by SDS-PAGE analyses also uncovered differences between the two types of amastigotes, especially among their respective set of proteins. Therefore, our work suggests that the morphological transformations of *T. cruzi* may serve as a robust model system to study the molecular mechanisms of morphological control.

Our results show that the pH-induced transformation of tissue-derived trypomastigotes previously reported by Tomlinson et al. (1995) was also observed using a different acidic medium. The parasites transformed into amastigotes at 18 to 24 h after incubation in MEMTAU medium at 37°C indicating a faster differentiation rate than previously reported (Andrews et al. 1987, Tomlinson et al. 1995). However, the transformation process of trypomastigotes adhered to the morphological patterns described by Andrews et al. (1987). It is very likely that the accelerated morphological changes observed must be accompanied by antigenic changes, since we could observe by Western blots with stage-specific antisera changes in antigen profiles (unpublished results). An advantage of our system is that the elapsed time is shorter and the transformation process is highly synchronized.

Recently, we have also shown by light microscopy, SDS-PAGE and Western blots that pre-incubation at 37°C of metacyclic trypomastigotes in MEMTAU medium triggered, 24 h after incubation, early transformation events such as an accelerated macromolecular differentiation to amastigotes without noticeable morphological changes. Late transformation events which occurred when the culture medium is changed, however, were characterized by profound morphological rearrangements with few molecular changes (Contreras et al. 2002). The data presented here provide a more detailed morphological analysis of the parasites during the pre-incubation and re-incubation phases. The images indicate that within 24 h after incubation, the metacyclic trypomastigotes exhibit a lengthening followed by a shortening of the body as the pre-incubation time progresses. We postulate that the apparent enlargement of the parasite may be the result of a progressive shedding of its posterior surface as a compaction process probably driven by changes in the rate of shortening of microtubules and which is faster than the compaction of the cellular membrane occurs (Karp 1999). Such mechanism may explain the loss of massive surface membrane observed right before and during the start of the rounding process as breaking during this transition was often observed. Concomitantly, a released of fine trails along the entire surface of the parasite was observed which could be associated with the sequential expression and loss of specific membrane antigens as previously reported by other authors (Andrews et al. 1987, Zeledon et al. 1988, Barros et al. 1996).

The observation that the first morphological events induced by pre-incubation are a transient lengthening of the posterior end of the metacyclic form, an apparent shift of the kinetoplast, and a thinning of the parasite body resulting from a slight unfolding of the undulating membrane, seem to indicate that an extensive cytoskeleton remodeling associated with high turnover of surface membrane may be taking place. It is conceivable that MAPs which connect the subpellicular microtubules to the plasma membrane may participate in this process (Gull 1999). Whether the early morphological changes and the "escaping" of the metacyclic trypomastigote from endocytic

vacuoles are causally related is unknown. It is noteworthy, however, that the transformation process can be continued and completed only after renewed the incubation medium. Assays to examine whether the product release from the parasite during pre-incubation phase, are involved in the inhibition of the morphological transformation are in progress and might be useful to explain why the metacyclic trypomastigote can also escape from endocytic vacuole into the host cell cytoplasm (Dvorak 1975).

Tyler and Engman (2000) have shown that the depletion of glucose from the medium triggers elongation of the epimastigotes flagellum. Later, the authors proposed that the intracellular glucose concentration is the key factor for both elongation of the flagellum and sustaining the differentiation of the metacyclic trypomastigote (Tyler & Engman 2001). In agreement with these data, we observed that the lengthening or shortening process exhibited during the pre-incubation phase is not accompanied by elongation of the metacyclic trypomastigote flagellum. On the contrary, a thick and very short free flagellum edging the body of the parasite was noted, as expected for incubation of parasites in a glucose-rich medium.

The most striking cellular rearrangement of the parasites occurred when the culture medium was changed. The sudden shortening and the blunting of the posterior end observed in the metacyclic trypomastigote within the first 8 h after re-incubation provides clues as to the dynamics of posterior region release during amastigogenesis. The subsequent morphological changes involving thickening of the posterior end and progressive shortening of the parasite around itself in a helical fashion, along with a gradual internalization of the flagellum resemble the changes for tissue-culture-derived trypomastigotes as described above. The fact that early and late morphological changes are associated with the different environmental conditions surrounding extracelullar primary amastigogenesis may provide an opportunity to study the role of ubiquitin (UB)-proteosome system, which was recently shown to be involved in the remodeling process of trypomastigote transformation (De Diego et al. 2001). It is worth noting that the early events described during primary amastigogenesis were not observed when tissue-culture derived trypomastigotes transformed into amastigotes. These morphological differences may indicate that the metacyclic form possesses a specific way of responding and adapting to environmental changes that is distinct from that shown by bloodstream trypomastigotes.

It has been reported that while the transformation of trypomastigotes is triggered by Phosphatidylinositol-Specific Phospholipase C (PI-PLC), the metacyclic forms are not affected (Mortara et al. 2001). In addition, the pH-induced transformation of tissue-derived trypomastigotes is not observed when metacyclic trypomastigotes are incubated under the same conditions (Tyler & Engman 2001). Interestingly, it is known that the first intracellular cycle of metacyclic trypomastigotes is significantly shorter than the cycle of tissue-culture-derived trypomastigotes of the same strain that has been growing as an obligate intracellular parasite for several cycles (Dvorak 1975). These differences may be explained by the fact that even though ETA and EMA may appear to be undistinguishable at the gross morphological level, they nevertheless display noticeable differences at the ultrastructural and molecular levels. For instance, under the scanning electron microscope, ETA exhibit a finely grained surface while EMA present a rough membrane surface. Furthermore, when their polypeptide and glycopeptides profiles were compared, we detected significantly different protein profiles between the two forms of amastigotes, suggesting that the ultrastructural differences found in ETA and EMA are underscored by differences in macromolecular constitution (Ruiz et al. 1993, Burleigh & Andrews 1995).

It is noteworthy that the intracellular amastigotes showed similar gross morphology, yet their crack patterns were different. Whether or not such difference is related to distinct biological properties is unknown, but may reflect differences in their development. Analogy can be made with works on human plasmodia (Aikawa & Atkinson 1990, Rey 1991, Bannister et al. 2000), where it has been described that the processes of shizogony occurring in the vertebrate host yield exoerythrocytic merozoites and erythrocyte merozoites with similar biological capacities, but with partly different morphologies and antigenicities. Thus, it is tempting to speculate that the IMA may be the parasitological equivalent to exoerythrocytic merozoites derived from infective sporozites transmitted by the vector insect, while the ITA may be equivalent to the erythrocyte merozoites. If so, one would expect that primary and secondary amastigogenesis in the vertebrate host will be different as well.

In conclusion, this paper reports on the first morphological comparison of the developmental processes giving rise to in vitro amastigotes from trypomastigote and metacyclic forms. Although it is clear that axenic amastigogenesis cannot mimic intracellular amastigogenesis in absolute terms, the data presented here demonstrates the utility of our experimental system as a model in which to begin the molecular study of parasite development in vivo. The ultrastructural and molecular differences observed between seemingly identical amastigotes (ETA and EMA) intimate that the mechanisms controlling primary and secondary intracellular amastigogenesis in *T. cruzi* may be different and should be investigated further.

ACKNOWLEDGEMENTS

To Dr Alejandro Sánchez Alvarado for helpful discussions and for his critical reading of the manuscript. To Rosa Y Arteaga for her assistance in parasite production. To Yunaimy Franco in processing electron microscopy sample. To Francy Duran, Gregorio Flores, Mr Wilmer Pineda, and Mr Johnny Albanese for excellent technical assistance.

REFERENCES

Aikawa M, Atkinson CT 1990. Immunoelectron microscopy of parasites. *Adv Parasitol 29*: 151-214.

Andrews NW, Hong K, Robbins ES, Nussenzweig V 1987. Stage-specific surface antigens expressed during the morphogenesis of vertebrate forms of *Trypanosoma cruzi*. *Exp Parasitol 64*: 474-484.

Bannister LH, Hopkins JM, Fowler RE, Krishna S, Mitchell GH 2000. A brief illustrated guide to the ultrastructure of *Plasmodium falciparum* asexual blood stages. *Parasitol Today 16*: 427-433.

Barros HC, Da Silva S, Verbisck NV, Araguth MF, Tedesco RC, Procopio DO, Mortara R 1996. Release of membrane-bound trail by *Trypanosoma cruzi* amastigotes onto modified surface and mammalian cells. *J Euk Microbiol 43*: 275-285.

Barros HC, Verbisck NV, Da Silva S, Araguth MF, Mortara R 1997. Distribution of epitopes of *Trypanosoma cruzi* amastigotes during the intracellular cycle within mammalian cells. *J Euk Microbiol 44*: 332-344.

Brener Z 1973. Biology of *Trypanosoma cruzi*. *Ann Rev Microbiol 27*: 347-382.

Burleigh BA, Andrews NW 1995. The mechanisms of *Trypanosoma cruzi* invasion of mammalian cells. *Annu Rev Microbiol 49*: 175-200.

Carvalho TMU, De Souza W 1983. Separation of amastigotes and trypomastigotes of *Trypanosoma cruzi* from culture cells. *Z Parasitenkd 69*: 571-73.

Carvalho TMU, De Sousa W 1989. Early event related with the behaviour of *Trypanosoma cruzi* within an endocytic vacuole in mouse peritoneal macrophages. *Cell Struct Funct 14*: 383-392.

Contreras VT, Araque W, Delgado V 1994. *Trypanosoma cruzi*: metacyclogenesis *in vitro*. I. Changes in the properties of metacyclic trypomastigotes maintained in the laboratory by different methods. *Mem Inst Oswaldo Cruz 89*: 253-259.

Contreras VT, Navarro MC, De Lima AR, Duran F, Arteaga R, Franco Y 2002. Early and late molecular and morphologic changes that occur during the *in vitro* transformation of *Trypanosoma cruzi* metacyclic trypomastigotes to amastigotes. *Biol Res 35*: 21-32**.**

De Diego JL, Katz JM, Marshall P, Gutierrez B, Manning JE, Nussenzweig V, Gonzalez J 2001. The ubiquitin-proteosome pathway plays an essential role in proteolysis during *Trypanosoma cruzi* remodeling. *Biochemistry 40*: 1053-1062.

De Moreno MR, Smith JF, Smith RV 1985. Silver staining of proteins in polyacrylamide gels: increased sensitivity through a combined blue-silver stain procedure. *Anal Biochem 151*: 466-470.

Dubray G, Bezard G 1982. A highly sensitive periodic acid-silver stain for 1,2-dol groups of glycoproteins and polysaccharides in polyacrylamide gels. *Anal Biochem 119*: 325-329.

Dvorak JA 1975. New *in vitro* approach to quantitation of *Trypanosoma cruzi*-vertebrate cell interaction. In New Approaches in American Trypanosomiasis Research. *PAHO Sci Publ 318*: 109-145.

Gull K 1999. The cytoskeleton of trypanosomatid parasites *Annu Rev Microbiol 53*: 629-655.

Kambara H, Uemura H, Nakazawa S, Fukama T 1990. Effect of low pH on transformation of *Trypanosoma cruzi* trypomastigote to amastigote. *Japan J Parasitol 39*: 226-228.

Karp G 1999. The cytoskeleton and cell motility. In G Karp, *Cell and Molecular Biology*: *Concepts and Experiments*, 2nd ed., John Wiley & Sons, New York, p. 365.

Kimura E, Lay W, Fernandez J 1978. Extracellular *in vitro* evolution of metacyclic trypomastigotes isolated from *Trypanosoma cruzi* culture. *Rev Inst Med Trop São Paulo 20*: 133-138.

Laemmli UK 1970. Cleavage of structural proteins during the assembly of the head of bacteriophage T4. *Nature* (London) *227*: 680-685.

Ley V, Andrews NW, Robbins ES, Nussenzweig V 1988. Amastigotes of *Trypanosoma cruzi* sustain an infective cycle in mammalian cells. *J Exp Med 168*: 649-59.

Ley V, Robbins ES, Nussenzweig V, Andrews NW 1990. The exit of *Trypanosoma cruzi* from the phagosome is inhibited by raising the pH of acidic compartments. *J Exp Med 171*: 401-413.

Milder R, Kloetzel J, Deane MP 1977. Observation on the interaction of peritoneal macrophages with *Trypanosoma cruzi*. II. Intracellular fate of bloodstream forms. *Rev Inst Med Trop São Paulo 19*: 313-322.

Moller HJ, Heinegard D, Poulsen JH 1993. Combined alcian blue silver stain of subnanogram quantities of proteoglycans and sulfate-polyacrylamide gels. *Anal Biochem 209*: 169-175.

Moller HJ, Poulsen JH 1995. Improved method for silver staining of glycoproteins in thin sodium dodecyl sulfate polyacrylamide gels. *Anal Biochem 266*: 371-374.

Mortara RA, Minelli LMS, Vandekerckhove F, Nussenzweig V, Juarez Ramallo-Pinto F 2001. Phosphatidylinositol-specific phospholipase C (PI-PLC) cleavage of GPI-anchored surface molecules of *Trypanosoma cruzi* triggers in vitro morphological reorganization of trypomastigotes. *J Euk Microbiol 48*: 27-37.

Nogueira N, Cohn ZA 1976. *Trypanosoma cruzi*: mechanism of entry and intracellular fate in mammalian cells. *J Exp Med 143*: 1402-1420.

Pan SC 1978. *Trypanosoma cruzi*: intracellular stages grown in a cell-free medium at 37°C. *Exp Parasitol 45*: 215-24.

Piras MM, Piras R, Henriquez D 1982. Changes in morphology and infectivity of cell culture-derived trypomastigotes of *Trypanosoma cruzi* fibroblasts. *Mol Biochem Parasitol 6*: 67-81.

Rey L 1991. Os plasmódios e a malária: I. Os Parasitos. In L Rey, *Parasitologia*, 2nd ed., Guanabara Koogan, Rio de Janeiro, p. 286-297.

Rondinelli E, Silva R, Carvalho JFO, Soares CMA, De Carvalho EF, De Castro FT 1988. *Trypanosoma cruzi:* an *in vitro* cycle of cell differentiation in axenic culture. *Exp Parasitol 66*: 197-204.

Ruiz RC, Rigoni VL, Gonzalez J, Yoshida N 1993. The 35/50 kDa surface antigen of *Trypanosoma cruzi* metacyclic trypomastigote, an adhesion molecule involved in host cell invasion. *Parasit Immunol 15*: 121-125.

Tardieux I, Webster P, Ravesloot J, Boron W, Lunn JA, Heuser JE, Andrews NW 1992. Lysosome recruitment and fusion are early events required for trypanosome invasion of mammalian cells. *Cell 71*: 1117-1126.

Tomlinson S, Vandekerchove F, Frevert U, Nussenzweig V 1995. The induction of *Trypanosoma cruzi* trypomastigote to amastigote transformation by low pH. *Parasitology 110*: 547-554.

Tyler KM, Engman DM 2000. Flagellar elongation induced by glucose limitation is preadaptative for *Trypanosoma cruzi* differentiation. *Cell Motil Cytoskeleton 46*: 269-278.

Tyler KM, Engman DM 2001. The life cycle of *Trypanosoma cruzi* revisited. *Int J Parasitol 31*: 472-481.

Villalta F, Kierzenbaum F 1982. Growth of isolated amastigotes of *Trypanosoma cruzi* in cell-free medium. *J Protozool 29*: 570-576.

Zeledon R, Bolaños R, Espejo Navarro MR, Rojas M 1988. Morphological evidence by scanning microscopy of excretion of metacyclic forms of *Trypanosoma cruzi* in vector's urine. *Mem Inst Oswaldo Cruz 83*: 361-365.